

# Monitoring statistics of the ERS-2 scatterometer for ESA

## Cycle 159

(Project Ref. 22025/08/I-EC)

Hans Hersbach  
European Centre for Medium-Range Weather Forecasts,  
Shinfield Park, Reading, RG2 9AX, England  
Tel: (+44 118) 9499476, e-mail: dal@ecmwf.int

August 11, 2010

## 1 Introduction

The quality of the UWI product was monitored at ECMWF for Cycle 159. Results were compared to those obtained from the previous Cycle, as well for data received during the nominal period in 2000 (up to Cycle 59). No corrections for duplicate observations from overlapping ground stations were applied.

During Cycle 159 data was received between 21:08 UTC 5 July 2010 and 20:28 UTC 9 August 2010. Data was grouped into 6-hourly batches (centred around 00, 06, 12 and 18 UTC). No data was received for the batches centred around 06 UTC and 18 UTC 6 July 2010, 06 UTC 18 July 2010, 18 UTC 27 July 2010, from 00 UTC 7 August 2010 to 06 UTC 8 August 2010, and for 06 UTC 9 August 2010.

Data is being recorded whenever within the visibility range of a ground station. For Cycle 159, data coverage was over the North-Atlantic, the Mediterranean, the Gulf of Mexico, a very small part of the Pacific west from the US, Canada and Central America, and the area in between Antarctica and Australia (see Figure 2). Compared to Cycle 158, a data gaps has appeared in the North Atlantic, no data was received over the Chinese Sea, while south of Australia coverage has improved.

For each day within Cycle 159, time series of the asymmetry between the fore and aft incidence angles consistently show large fluctuations around 12 UTC. In retrospect, the onset of this not previously observed behaviour seems to occur mid-way Cycle 158.

Compared to Cycle 158, the UWI wind speed relative to ECMWF first-guess (FG) fields showed a reduced standard deviation (1.30 m/s, was 1.33 m/s). Bias levels were more negative (on average -1.14 m/s, was -1.08 m/s).

Ocean calibration shows that inter-node and inter-beam dependencies of bias levels are similarly large. Average bias levels were less negative (-0.87 dB, was -0.98 dB; see Figure 4).

The ECMWF operational assimilation and forecast system was not changed during Cycle 159.

The Cycle-averaged evolution of performance relative to ECMWF first-guess (FG) winds is displayed in Figure 1. Figure 2 shows global maps of the over Cycle 159 averaged UWI data coverage and wind climate, Figure 3 for performance relative to FG winds.

## 2 ERS-2 statistics from 5 July 2010 to 9 August 2010

### 2.1 Sigma0 bias levels

The average sigma0 bias levels (compared to simulated sigma0's based on ECMWF model FG winds) stratified with respect to antenna beam, ascending or descending track and as function of incidence angle (i.e. across-node number) is displayed in Figure 4.

Compared to Cycle 158, inter-node and inter-beam dependencies between the fore and aft are similarly large. Average bias level was less negative (-0.87 dB, was -0.98 dB), being 0.5 dB more negative than for nominal data in 2000 (around -0.4 dB; see Figure 1 of the reports for Cycle 48 to 59). The situation is similar to that of one year ago (see report for Cycle 149).

Long-term variations correlate with the yearly cycle, which, given the non-global coverage, is understandable. Therefore, the method of ocean calibration will probably only provide accurate information on calibration levels for globally or yearly averaged data sets.

The data volume of descending tracks was about 55% lower than for ascending tracks.

### 2.2 Incidence angles

From simple geometrical arguments it follows that variations in yaw attitude will lead to asymmetries between the incidence angles of the fore and aft beam. Indeed, this has been observed. Figure 5 gives a time evolution of this asymmetry. Also in this Figure, the occasions for which the combined  $k_p$ -yaw quality flag was set are indicated by red stars. The relation with incidence-angle asymmetries is obvious.

The asymmetry between the fore and aft incidence angles shows large peaks, which consistently occur around 12 UTC for every single day of Cycle 159. This behaviour has not been observed before.

After a prolonged minimum, solar activity is on the rise. Around 27 July 2010 and 3 August 2010, solar wind caused a geomagnetic storm (source: [www.spaceweather.com](http://www.spaceweather.com)). These events did not seem to have an effect on ERS-2 attitude control.

## 2.3 Distance to cone history

The distance to the cone history is shown in Figure 6. Curves are based on data that passed all QC, including the test on the  $k_p$ -yaw flag, and subject to the land and sea-ice check at ECMWF (see cyclic report 88 for details).

Like for previous Cycles, time series are (due to lack of statistics) very noisy, especially for the near-range nodes. Most spikes were found to be the result of low data volumes.

Compared to Cycle 158, the average level decreased (1.27, was 1.33), and is higher (by 17%) than for nominal data (see top panel Figure 1).

The fraction of data that did not pass QC is displayed in Figure 6 as well (dashed curves). From these it is seen that for each day a large fraction of data is rejected around 12 UTC, which corresponds to the large observed peaks in the asymmetry between the fore and aft beam incidence angles.

## 2.4 UWI minus First-Guess wind history

In Figure 7, the UWI minus ECMWF first-guess wind-speed history is plotted. The history plot shows a few peaks, which are usually the result of low data volume. A decrease in the negative relative bias near the end of Cycle 158 (see corresponding cyclic report) reverts to more usual levels after the first few days of Cycle 159.

Figure 11 displays the locations for which UWI winds were more than 8 m/s weaker (top panel), respectively more than 8 m/s stronger (lower panel) than FG winds. Like for Cycle 158, such collocations are isolated, and often indicate meteorologically active regions, for which UWI data and ECMWF model field show reasonably small differences in phase and/or intensity. Deviations near the poles are the result of imperfect sea-ice flagging.

Two cases for which UWI winds were considerably different from FG winds are presented in Figure 12. Both cases (top panel in the South Pacific and lower panel in the Tropical Atlantic) show suspicious patches of UWI winds that are more or less orthogonal to the satellite track.

Average bias levels and standard deviations of UWI winds relative to FG winds are displayed in Table 1. From this it follows that the bias of UWI winds was somewhat more negative (-1.14 m/s, was -1.08 m/s), being around -0.3 m/s more negative than for nominal data in 2000.

On a longer time scale seasonal bias trends are observed (see Figure 1). As was highlighted in previous cyclic reports, it is believed that the yearly trend is partly induced by changing local geophysical conditions.

The standard deviation of UWI wind speed versus ECMWF FG has, compared to Cycle 158, was reduced (1.30 m/s, was 1.33 m/s).

For Cycle 159 the (UWI - FG) direction standard deviations were mostly ranging between 20 and 40 degrees (Figure 8). An increased scatter and volatility as observed near the end of Cycle 158 reverts back to more nominal levels on 13 August 2010. Average STDV for UWI wind direction was lower than for Cycle 158 (24.7 degrees, was 28.7 degrees). For at ECMWF de-aliased winds (Figure 10) performance is (slightly) improved

	Cycle 158		Cycle 159	
	UWI	CMOD4	UWI	CMOD4
speed STDV	1.33	1.34	1.30	1.29
node 1-2	1.40	1.39	1.39	1.37
node 3-4	1.33	1.32	1.31	1.30
node 5-7	1.28	1.28	1.26	1.26
node 8-10	1.28	1.28	1.24	1.24
node 11-14	1.30	1.31	1.25	1.25
node 15-19	1.32	1.34	1.24	1.24
speed BIAS	-1.08	-1.09	-1.14	-1.15
node 1-2	-1.56	-1.55	-1.67	-1.65
node 3-4	-1.34	-1.31	-1.43	-1.40
node 5-7	-1.11	-1.10	-1.18	-1.17
node 8-10	-0.94	-0.95	-0.99	-1.00
node 11-14	-0.89	-0.92	-0.94	-0.98
node 15-19	-0.91	-0.95	-0.96	-1.01
direction STDV	28.7	18.4	24.7	17.4
direction BIAS	-2.1	-2.4	-0.8	-1.1

Table 1: Biases and standard deviation of ERS-2 versus ECMWF FG winds in m/s for speed and degrees for direction.

as well (STDV 17.4, was 18.4 degrees).

## 2.5 Scatterplots

Scatterplots of FG winds versus ERS-2 winds are displayed in Figures 13 to 16. Values of standard deviations and biases are slightly different from those displayed in Table 1. Reason for this is that, for plotting purposes, the in 0.5 m/s resolution ERS-2 winds have been slightly perturbed (increases scatter with 0.02 m/s), and that zero wind-speed ERS-2 winds have been excluded (decreases scatter by about 0.05 m/s).

The scatterplot of UWI wind speed versus FG (Figure 13) is very similar to that for (at ECMWF inverted) de-aliased CMOD4 winds (Figure 15). It confirms that the ESACA inversion scheme is working properly.

Winds derived on the basis of CMOD5 are displayed in Figure 16. The relative standard deviation is lower than for CMOD4 winds (1.26 m/s versus 1.32 m/s). Compared to ECMWF FG, CMOD5 winds are 0.68 m/s slower.

## Figure Captions

**Figure 1:** Evolution of the performance of the ERS-2 scatterometer averaged over 5-weekly Cycles from 12 December 2001 (Cycle 69) to 9 August 2010 (end Cycle 159) for

the UWI product (solid, star) and de-aliased winds based on CMOD4 (dashed, diamond). Results are based on data that passed the UWI QC flags. For Cycle 85 two values are plotted; the first value for a global set, the second one for a regional set (for details see the corresponding cyclic report). Dotted lines represent values for Cycle 59 (5 December 2000 to 17 January 2001), i.e. the last stable Cycle of the nominal period. From top to bottom panel are shown the normalized distance to the cone (CMOD4 only) the standard deviation of the wind speed compared to FG winds, the corresponding bias (for UWI winds the extremes in node-wise averages are shown as well), and the standard deviation of wind direction compared to FG.

**Figure 2:** Average number of observations per 12H and per 125km grid box (top panel) and wind climate (lower panel) for UWI winds that passed the UWI flags QC and a check on the collocated ECMWF land and sea-ice mask.

**Figure 3:** The same as Figure 2, but now for the relative bias (top panel) and standard deviation (lower panel) with ECMWF first-guess winds.

**Figure 4:** Ratio of  $\langle \sigma_0^{0.625} \rangle / \langle \text{CMOD4}(\text{FirstGuess})^{0.625} \rangle$  converted in dB for the fore beam (solid line), mid beam (dashed line) and aft beam (dotted line), as a function of incidence angle for descending and ascending tracks. The thin lines indicate the error bars on the estimated mean. First-guess winds are based on the in time closest (+3h, +6h, +9h, or +12h) T799 forecast field, and are bilinearly interpolated in space.

**Figure 5:** Time series of the difference in incidence angle between the fore and aft beam. Red stars indicate the occurrences for which the combined  $k_p$ -yaw flag was set.

**Figure 6:** Mean normalized distance to the cone computed every 6 hours for nodes 1-2, 3-4, 5-7, 8-10, 11-14 and 15-19). The dotted curve shows the number of incoming triplets in logarithmic scale (1 corresponds to 60,000 triplets) and the dashed one indicates the fraction of complete (based on the land and sea-ice mask at ECMWF) sea-located triplets rejected by ESA flags, or by the wind inversion algorithm (0: all data kept, 1: no data kept).

**Figure 7:** Mean (solid line) and standard deviation (dashed line) of the wind speed difference UWI - first guess for the data retained by the quality control.

**Figure 8:** Same as Fig. 7, but for the wind direction difference. Statistics are computed for winds stronger than 4 m/s.

**Figures 9 and 10:** Same as Fig. 7 and 8 respectively, but for the de-aliased CMOD4 data.

**Figure 11:** Locations of data during Cycle 159 for which UWI winds are more than 8 m/s weaker (top panel) respectively stronger (lower panel) than FG, and on which QC on UWI flags and the ECMWF land/sea-ice mask was applied.

**Figure 12:** Comparison of UWI winds (in red) with ECMWF FG winds (in blue) for a case on 14 July 2010 in the South Pacific (top panel) and a case on 6 August 2010 west of Cape Verde (lower panel).

**Figure 13:** Two-dimensional histogram of first guess and UWI wind speeds, for the data kept by the UWI flags, and QC based on the ECMWF land and sea-ice mask. Circles denote the mean values in the y-direction, and squares those in the x-direction.

**Figure 14:** Same as Fig. 13, but for wind direction. Only winds stronger than 4m/s are taken into account.

**Figure 15:** Same as Fig. 13, but for de-aliased CMOD4 winds.

**Figure 16:** Same as Fig. 13, but for de-aliased CMOD5 winds.

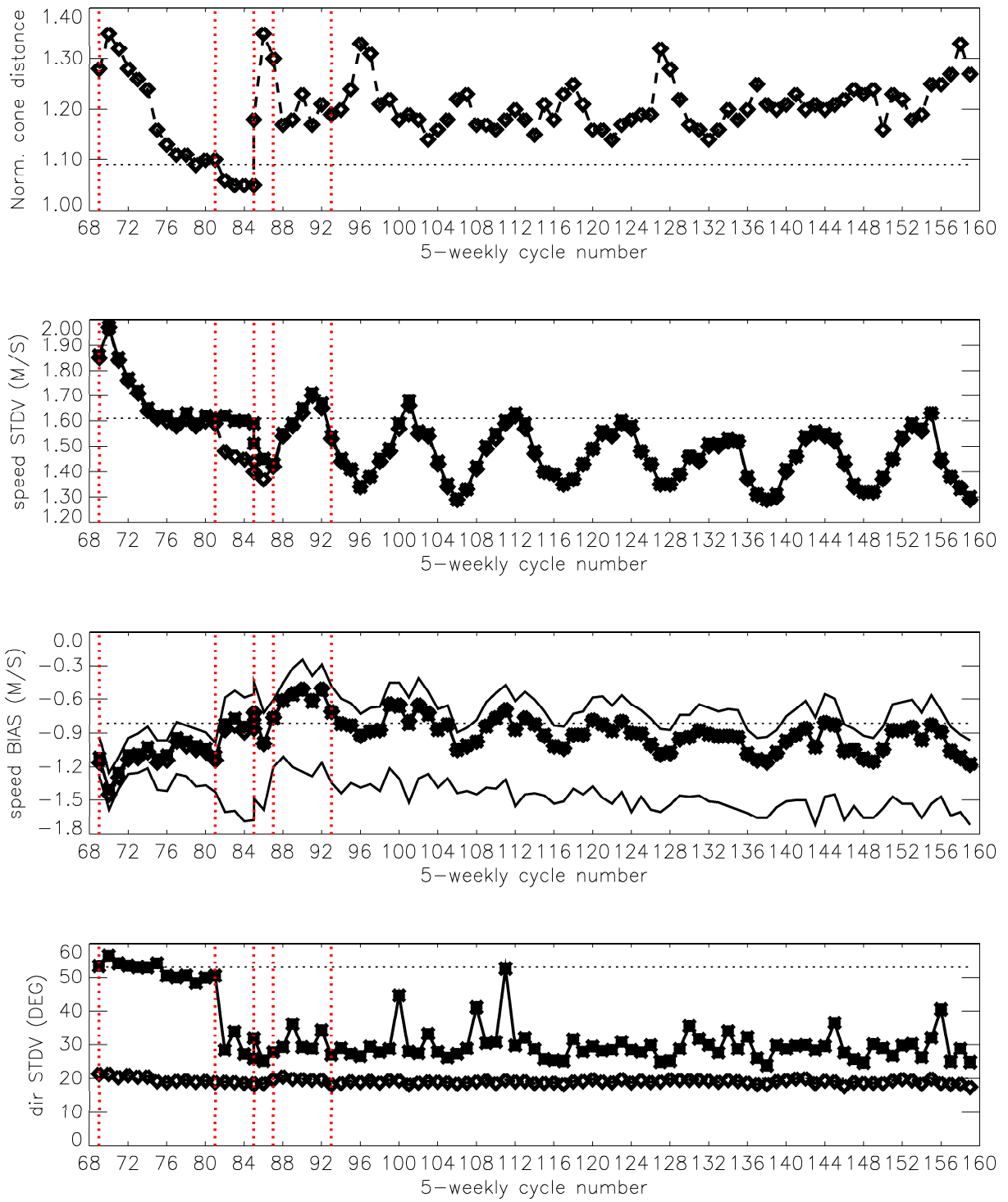
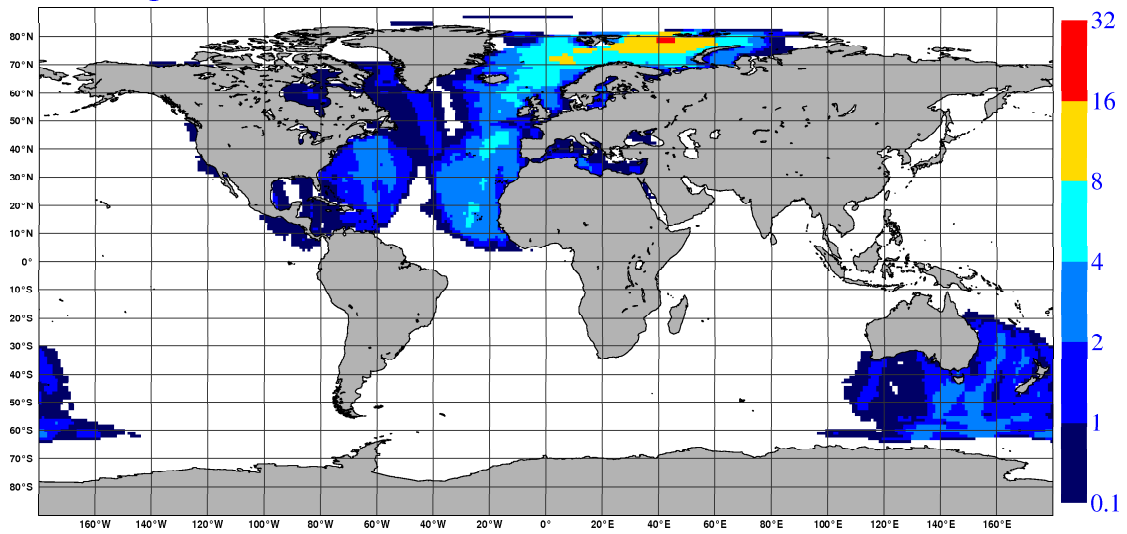


Figure 1

NOBS ( ERS-2 UWI ), per 12H, per 125km box  
average from 2010070600 to 2010080918 GLOB:1.64



AVERAGE ( ERS-2 UWI ), in m/s.  
average from 2010070600 to 2010080918 GLOB:6.4

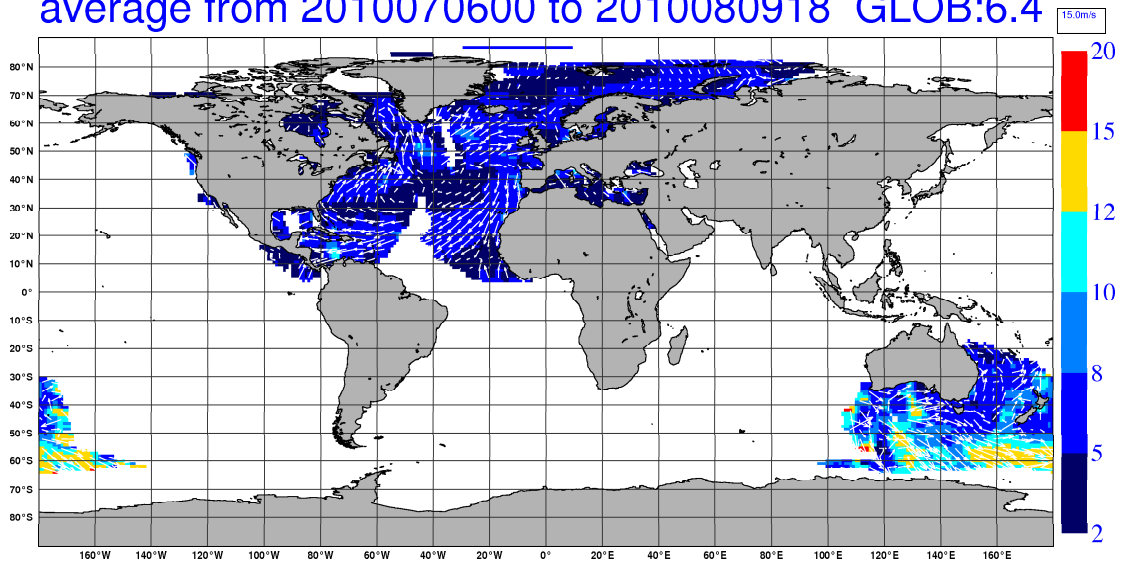
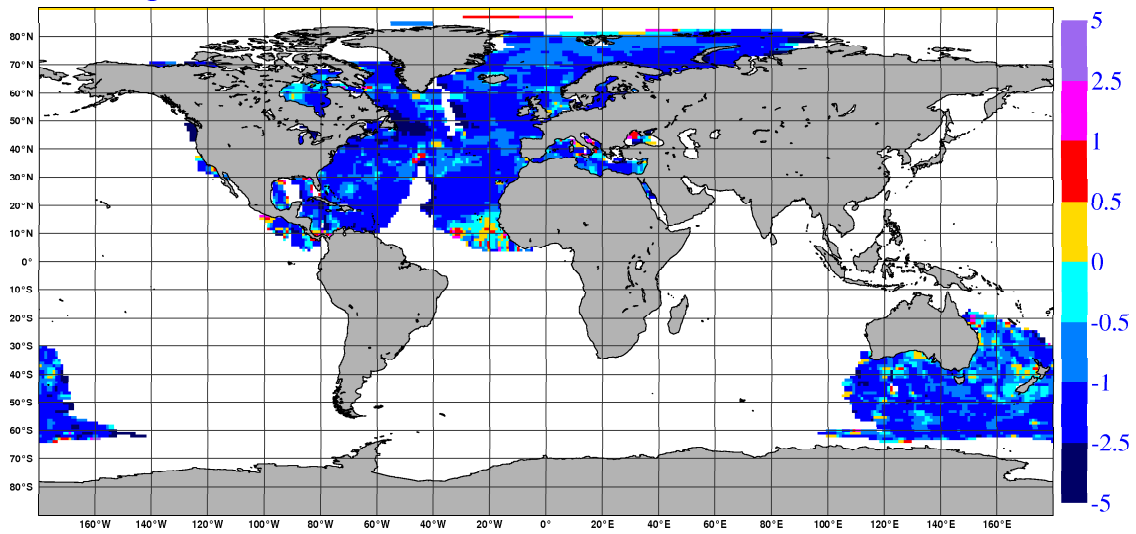


Figure 2



BIAS ( ERS-2 UWI vs FIRST-GUESS ), in m/s.  
average from 2010070600 to 2010080918 GLOB:-1.19



STDV ( ERS-2 UWI vs FIRST-GUESS ), in m/s.  
average from 2010070600 to 2010080918 GLOB:1.05

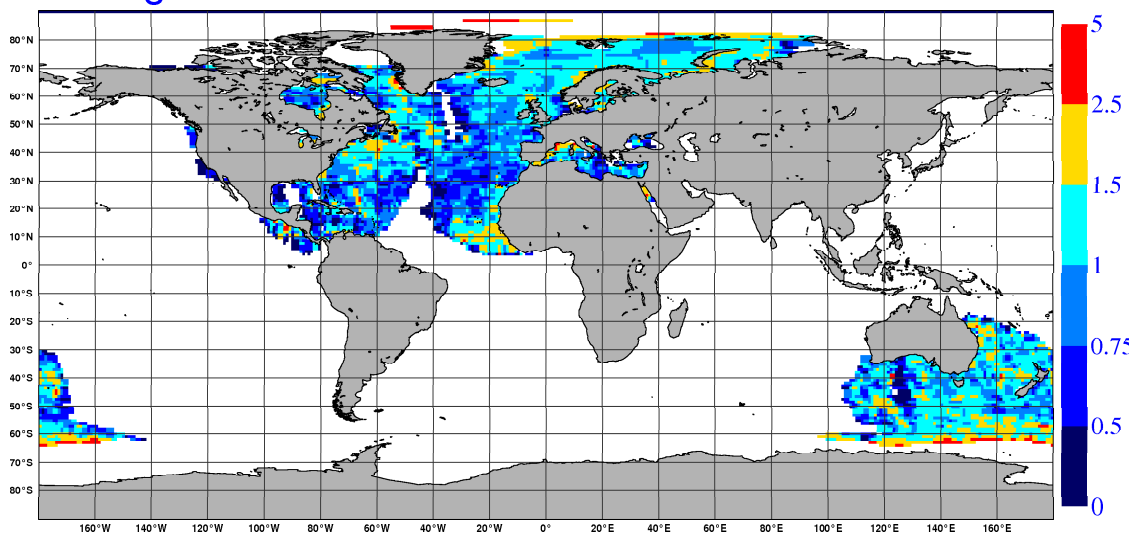
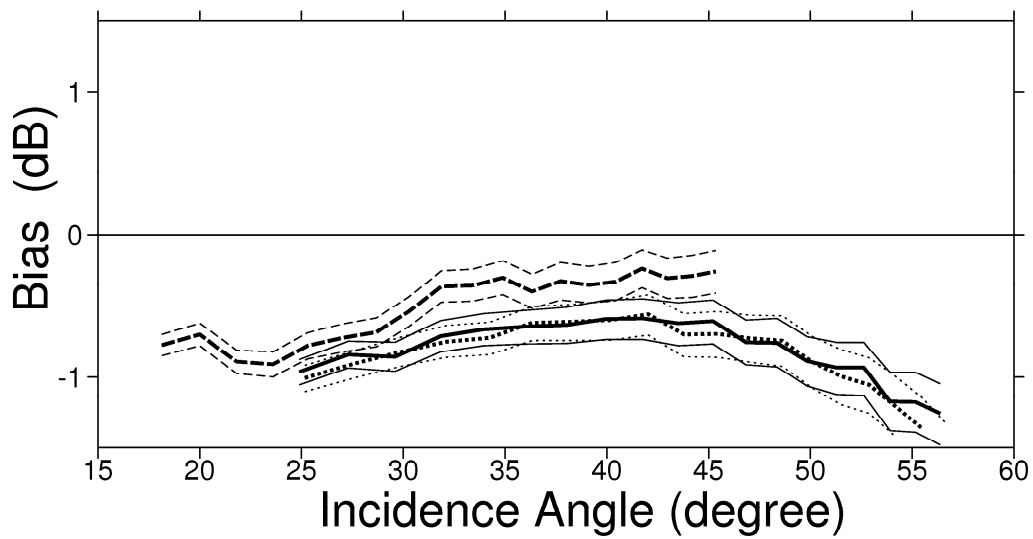


Figure 3

BIAS:  $(s_{0obs}^{**0.625}) / (s_{0fg3h}^{**0.625})$   
ERS-2 obs. from 05/07/2010 21:08 UTC to 09/08/2010 20:28 UTC  
DESCENDING TRACKS  
174708 Entries, 36.5 % used (flat wind dir. dist.)  
\_\_\_ Fore \_\_Mid ...Aft thin: Error Bar



BIAS:  $(s_{0obs}^{**0.625}) / (s_{0fg3h}^{**0.625})$   
ERS-2 obs. from 05/07/2010 21:08 UTC to 09/08/2010 20:28 UTC  
ASCENDING TRACKS  
394676 Entries, 59.3 % used (flat wind dir. dist.)  
\_\_\_ Fore \_\_Mid ...Aft thin: Error Bar

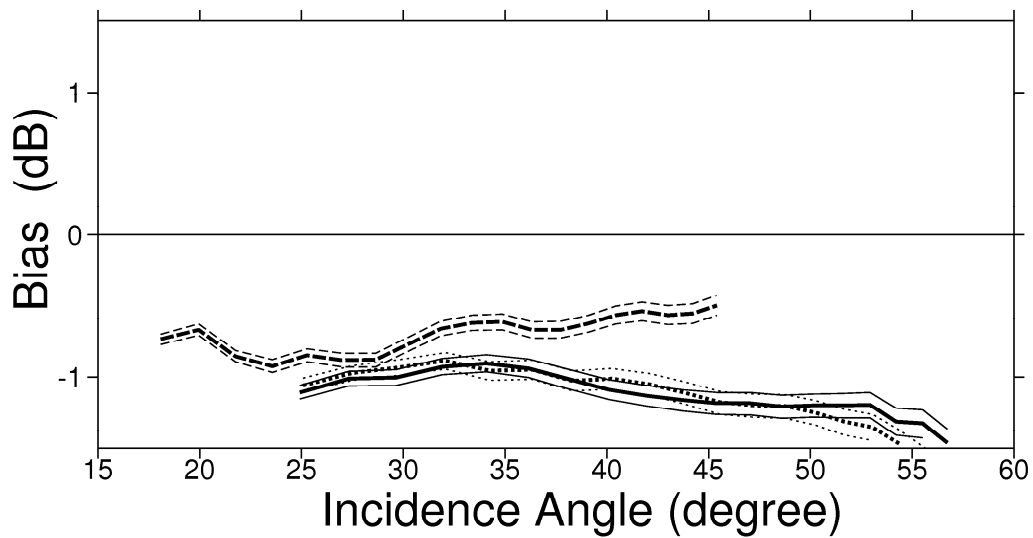


Figure 4

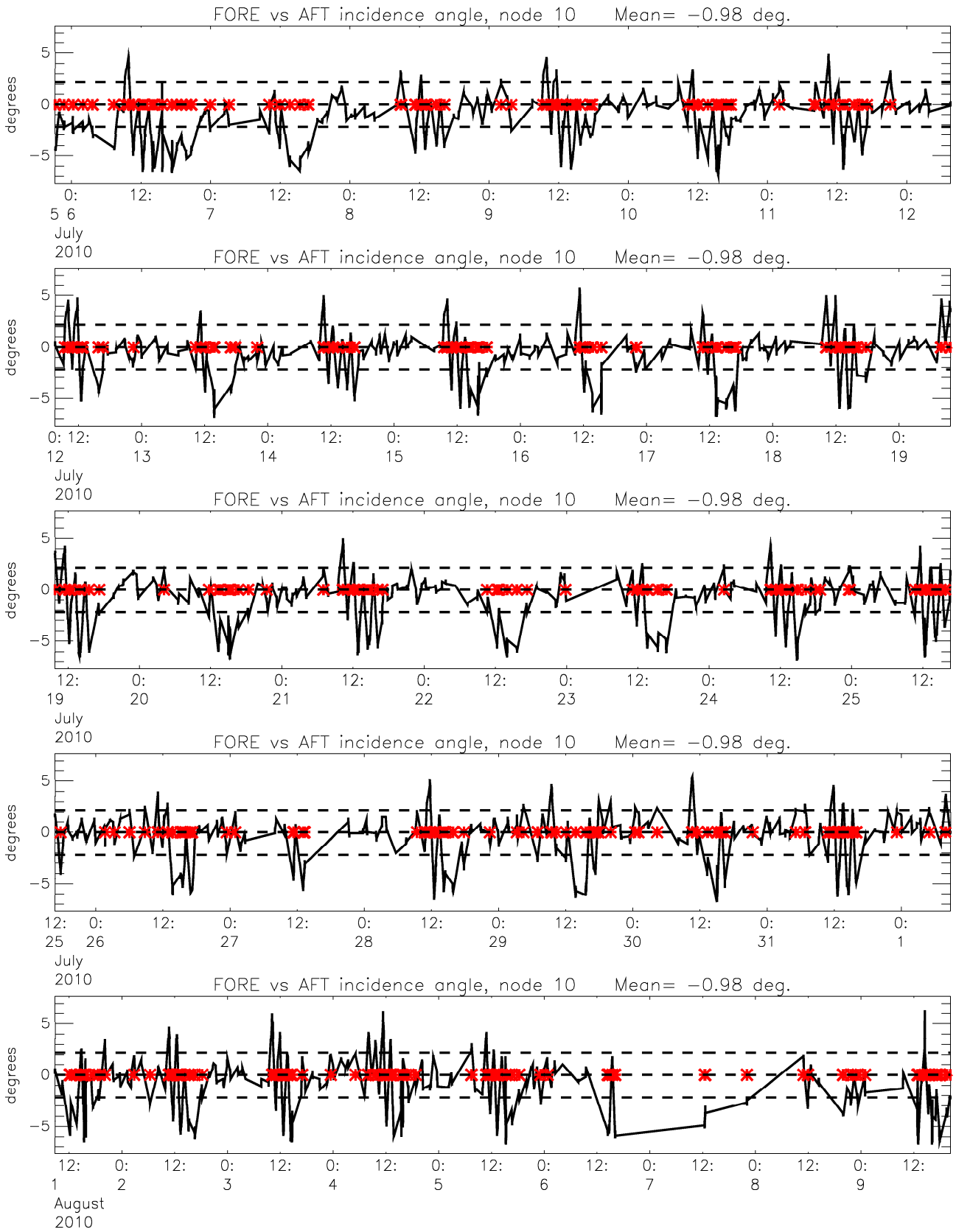


Figure 5

# Monitoring of Sigma0 triplets versus CMOD4 for ERS-2

from 2010070600 to 2010080918

(solid) mean normalised distance to the cone over 6 h

(dashed) fraction of complete sea-point observations rejected by ESA flag or CMOD4 inversion

(dotted) total number of data in log. scale (1 for 60000)

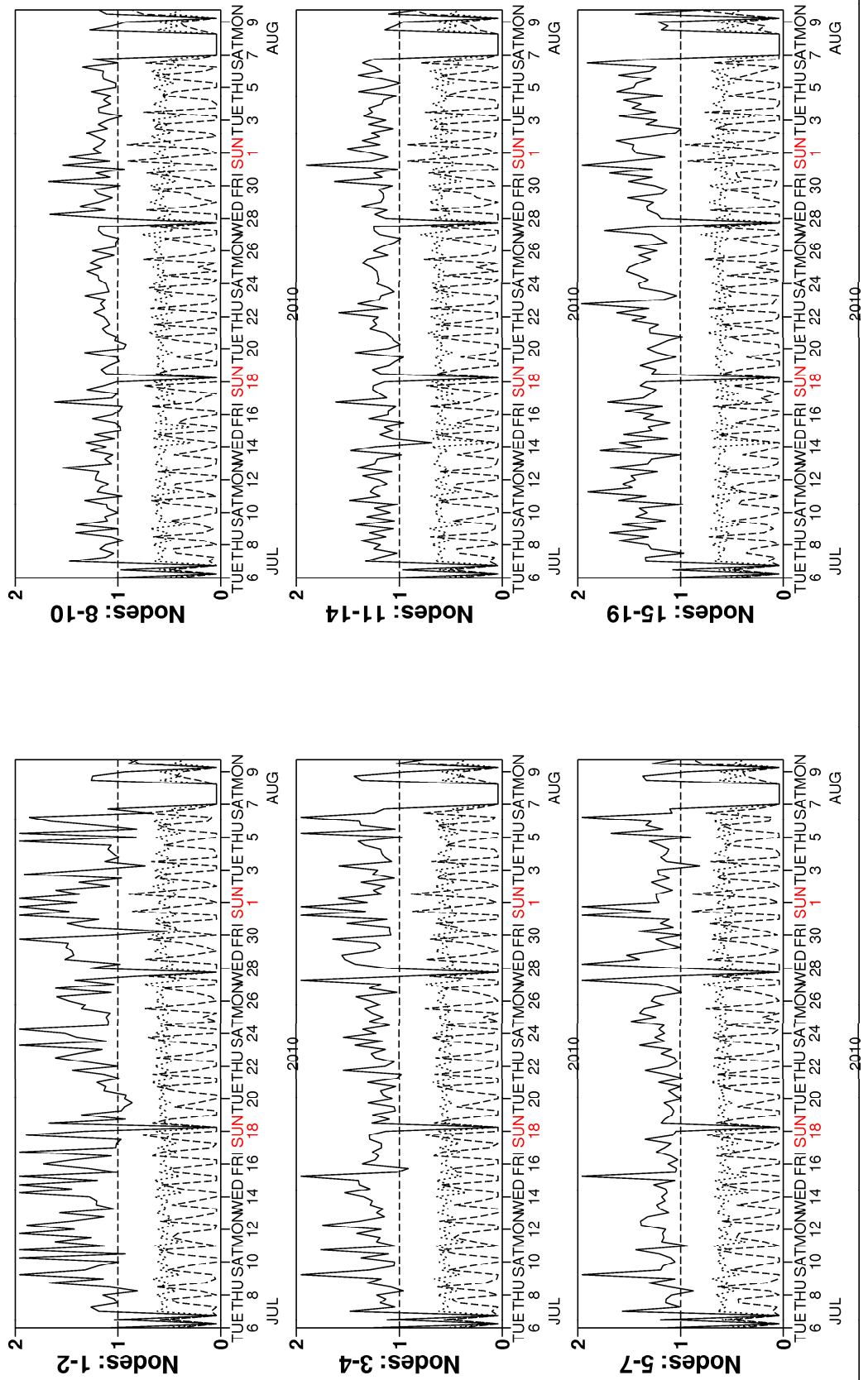


Figure 6

# Monitoring of UWI winds versus First Guess for ERS-2

from 2010070600 to 2010080918

(solid) wind speed bias UWI - First Guess over 6h (deg.)

(dashed) wind speed standard deviation UWI - First Guess over 6h (deg.)

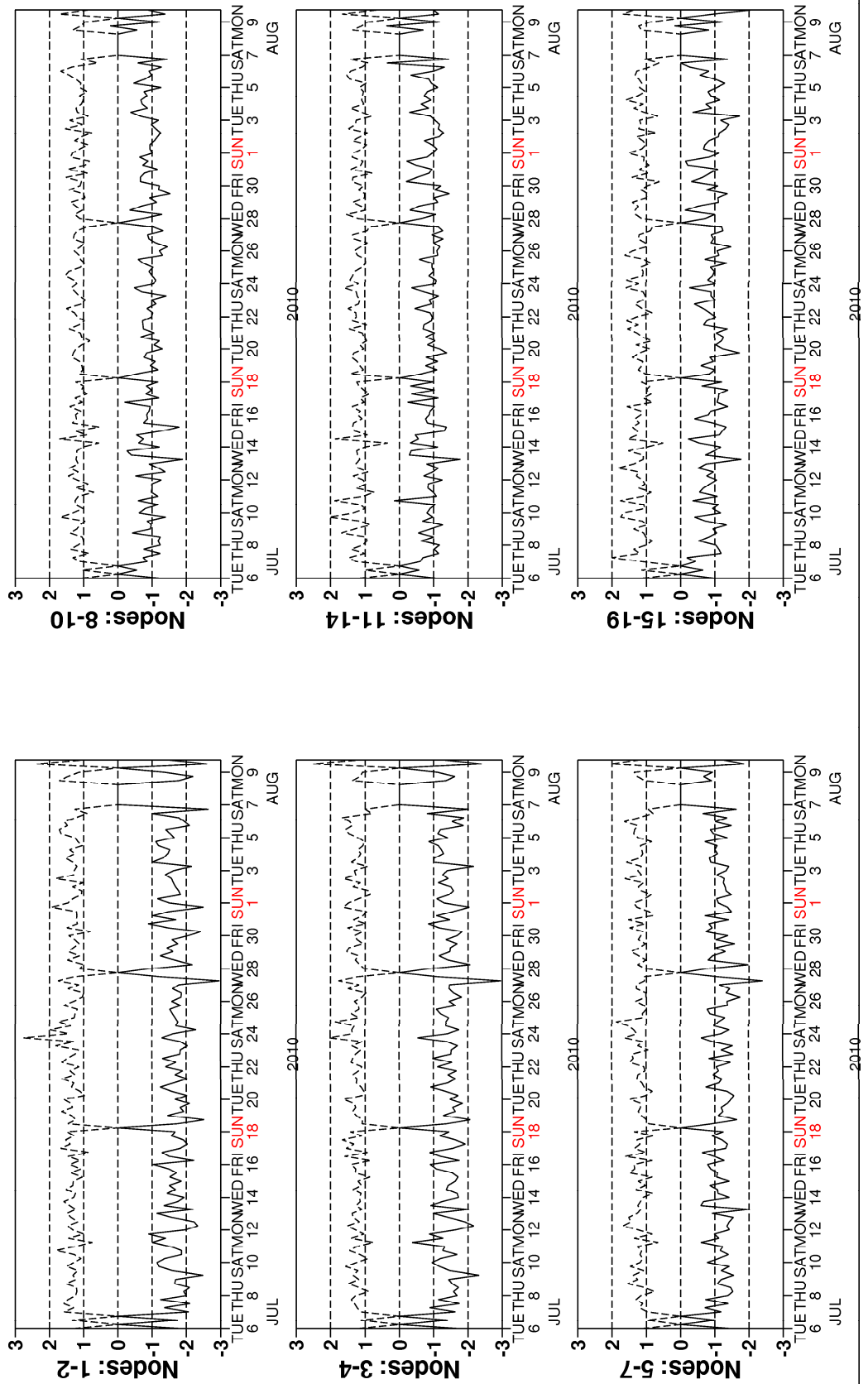


Figure 7

# Monitoring of UWI winds versus First Guess for ERS-2

from 2010070600 to 2010080918

(solid) wind direction bias UWI - First Guess over 6h (deg.)

(dashed) wind direction standard deviation UWI - First Guess over 6h (deg.)

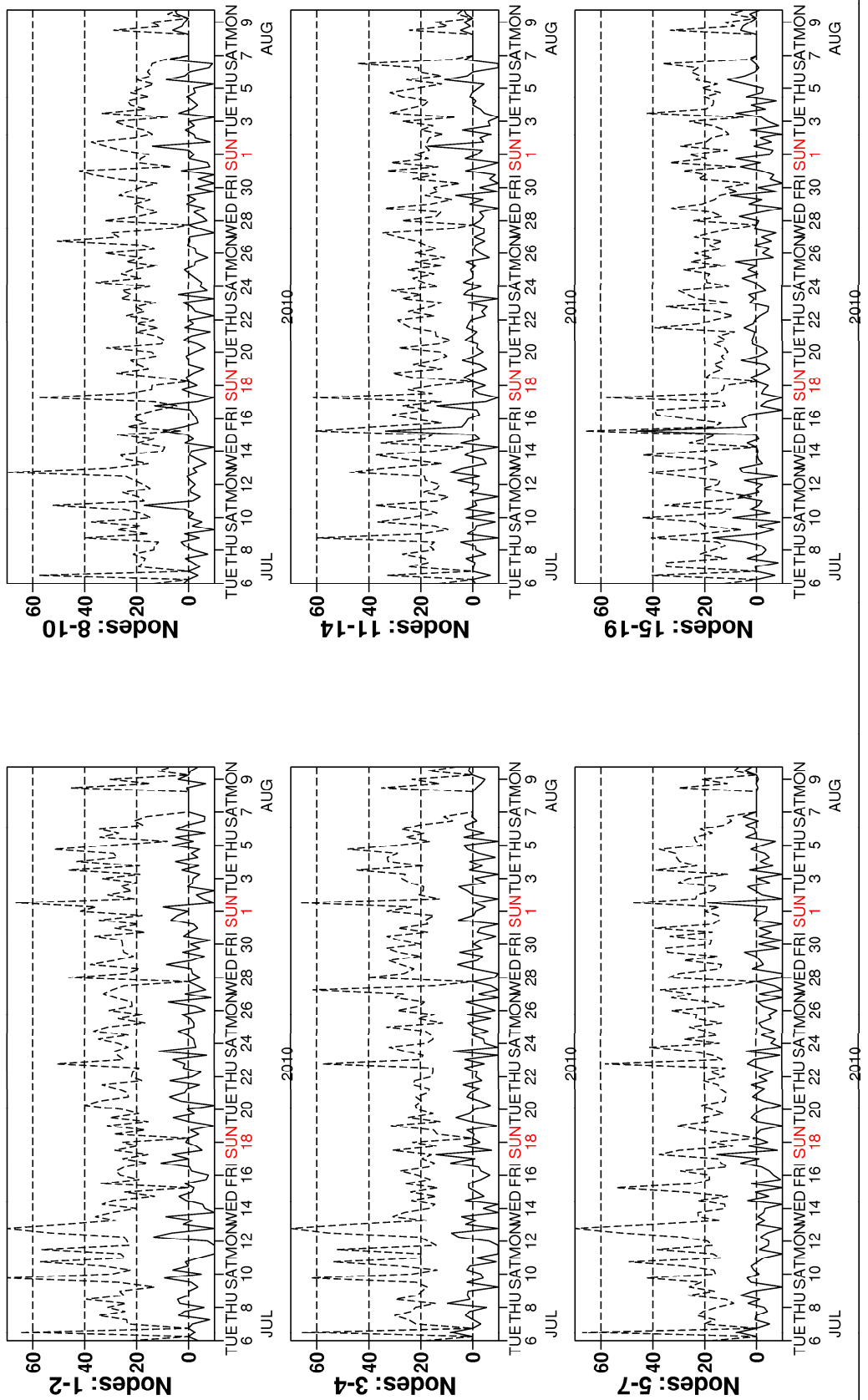


Figure 8

# Monitoring of de-aliased CMOD4 winds versus First Guess for ERS-2

from 2010070600 to 2010080918

(solid) wind speed bias CMOD4 - First Guess over 6h (deg.)

(dashed) wind speed standard deviation CMOD4 - First Guess over 6h (deg.)

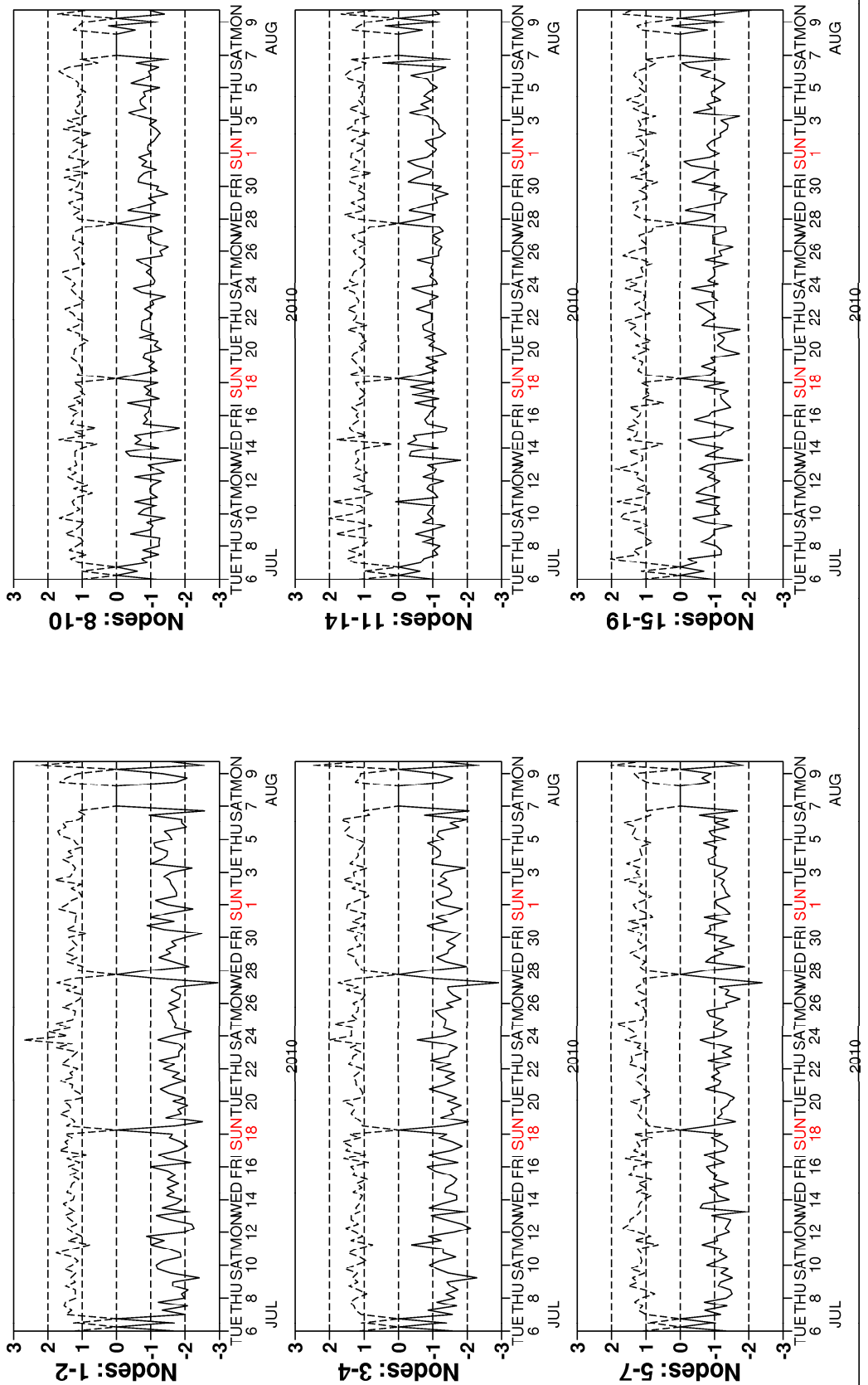


Figure 9

# Monitoring of de-aliased CMOD4 winds versus First Guess for ERS-2

from 2010070600 to 2010080918

(solid) wind direction bias CMOD4 - First Guess over 6h (deg.)

(dashed) wind direction standard deviation CMOD4 - First Guess over 6h (deg.)

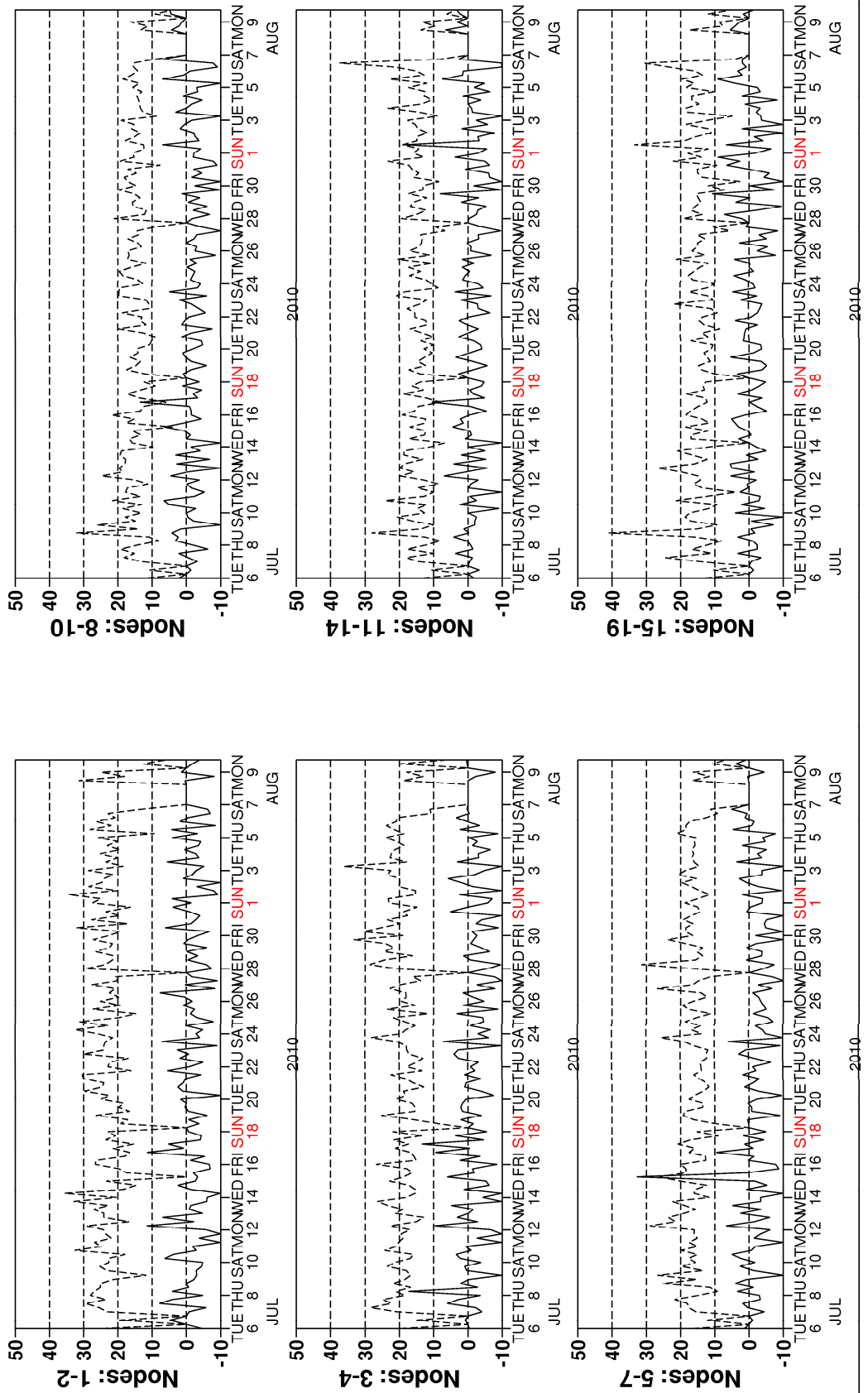
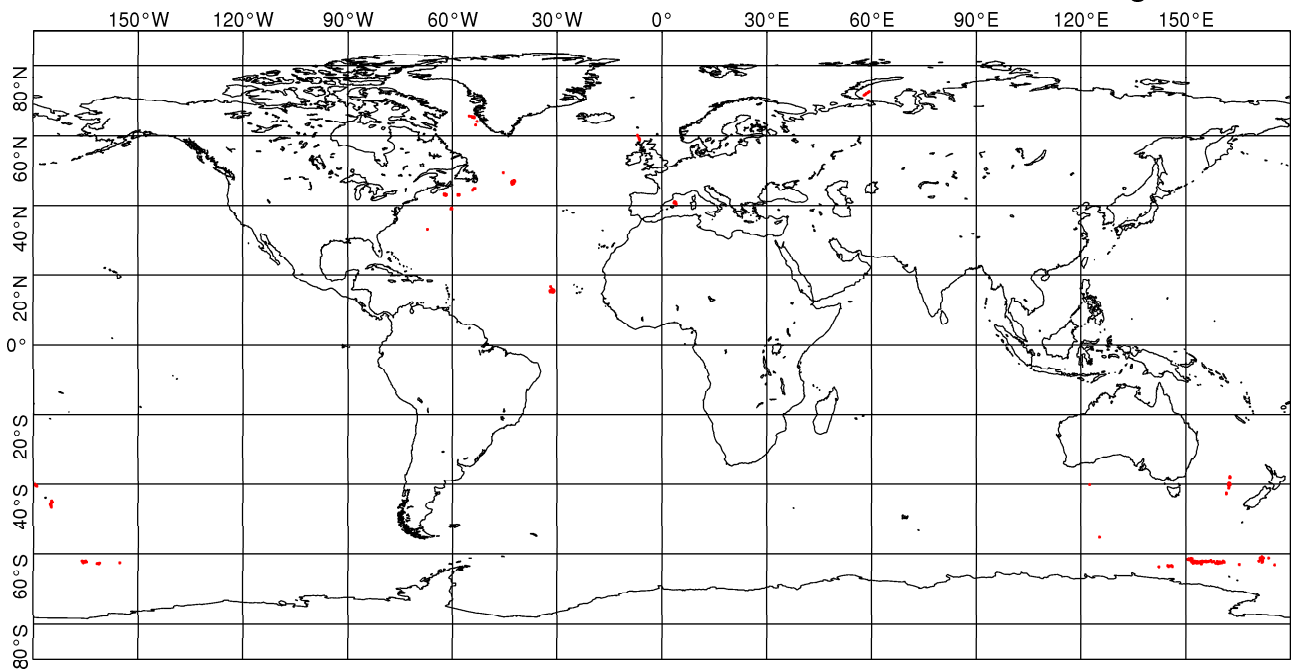


Figure 10



UWI winds more than 8 m/s weaker than ECMWF First Guess  
CYCLE 159, 2010070600 to 2010080918, QC on ESA flags



UWI winds more than 8 m/s stronger than ECMWF First Guess  
CYCLE 159, 2010070600 to 2010080918, QC on ESA flags

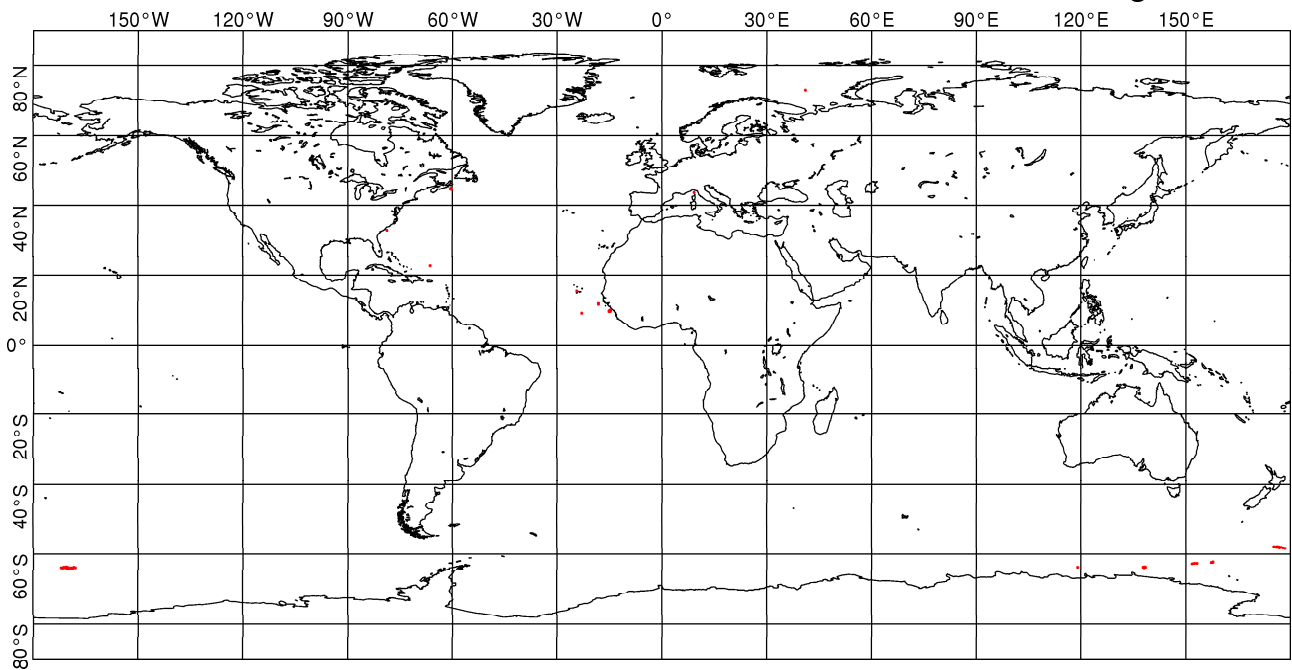
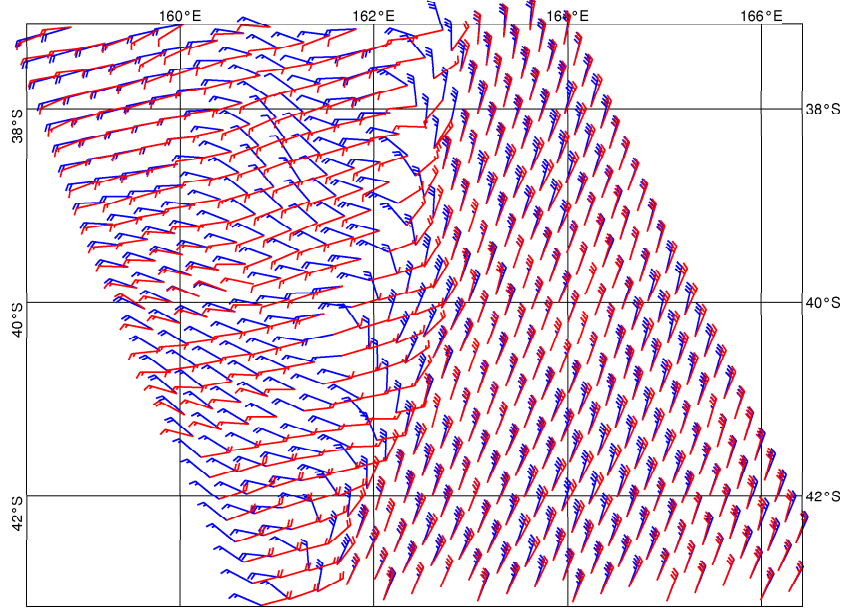


Figure 11

UWI winds (red) versus ECMWF FG winds (blue)  
South Pacific 20100714 12:31 UTC



UWI winds (red) versus ECMWF FG winds (blue)  
Cape Verde 20100806 00:40 UTC

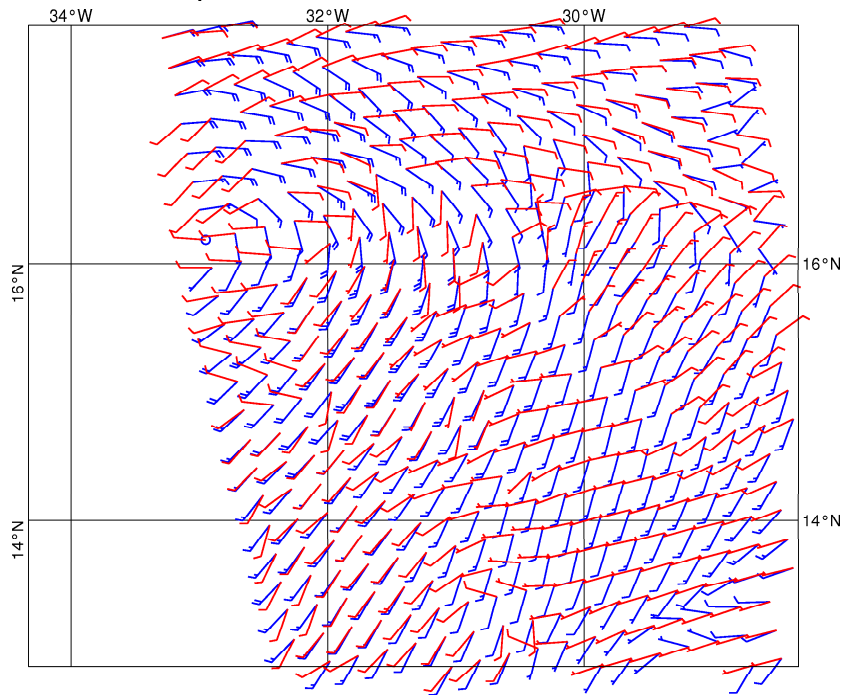


Figure 12

ECMWF 3-hourly First-Guess winds versus UWI winds  
from 2010070600 to 2010080918  
= 569384, db contour levels, 5 db step, 1st level at 2.6 db  
 $m(y-x) = -1.14$   $sd(y-x) = 1.32$   $sdx = 3.42$   $sd y = 3.11$   $pcxy = 0.960$

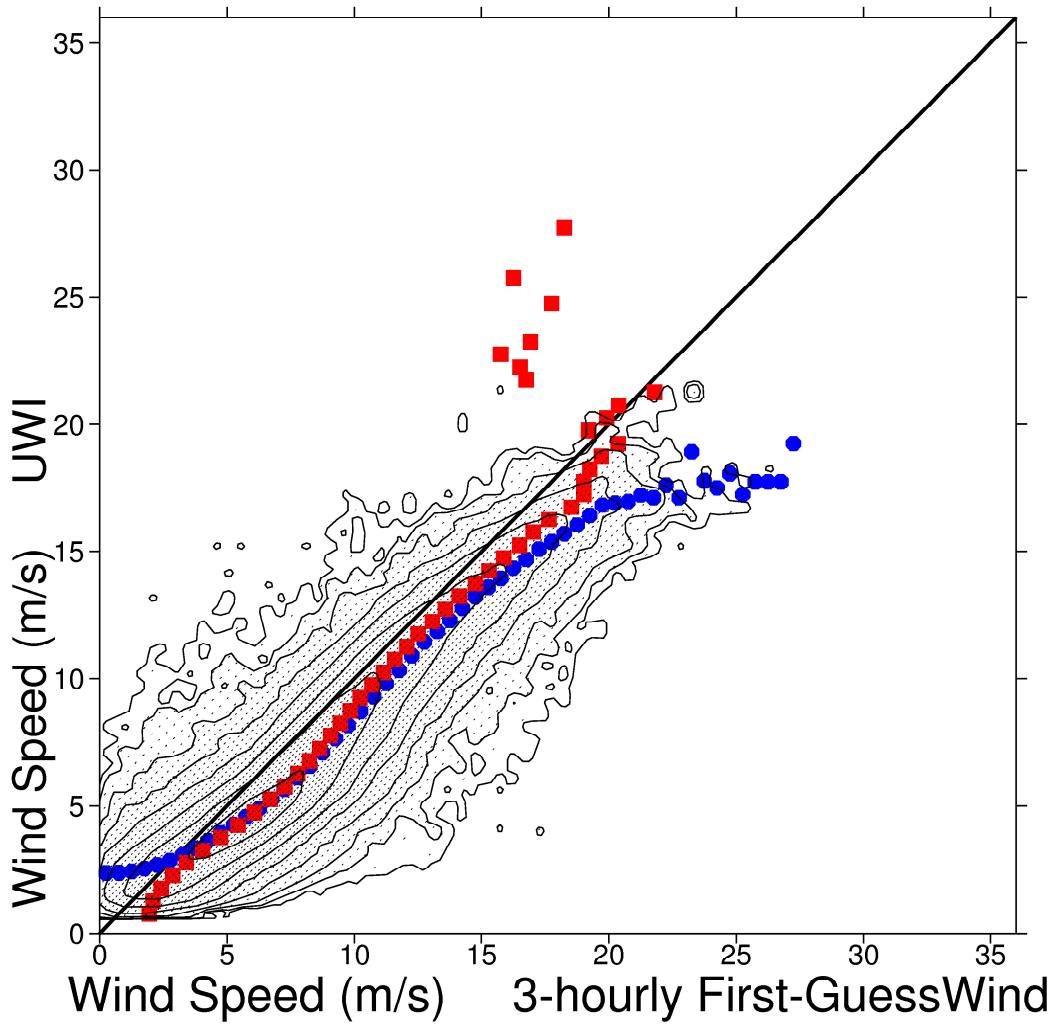


Figure 13

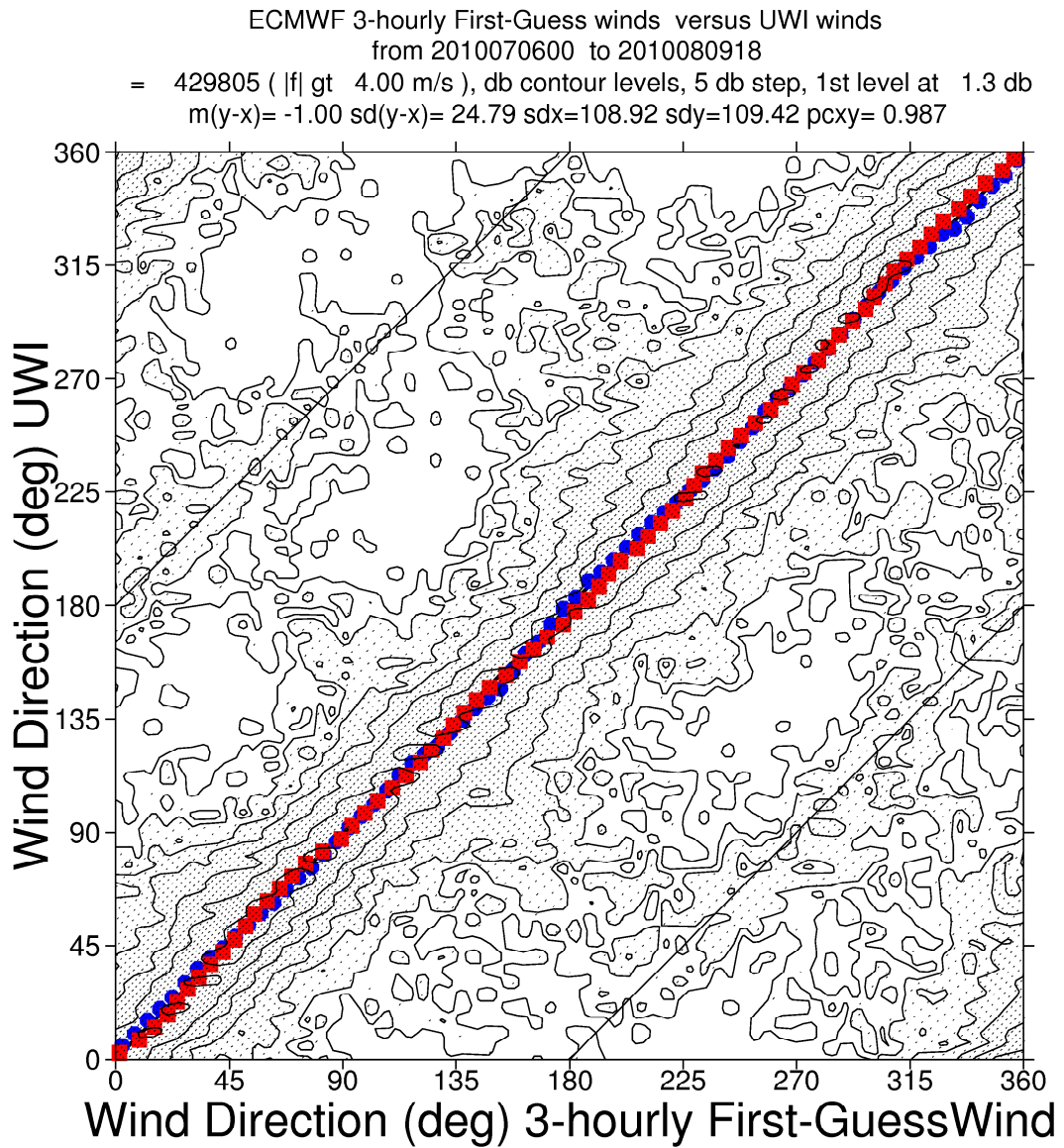


Figure 14

ECMWF 3-hourly First-Guess winds versus CMOD4 winds  
from 2010070600 to 2010080918  
= 560791, db contour levels, 5 db step, 1st level at 2.5 db  
 $m(y-x) = -1.15$   $sd(y-x) = 1.32$   $sdx = 3.39$   $sdy = 3.09$   $pcxy = 0.960$

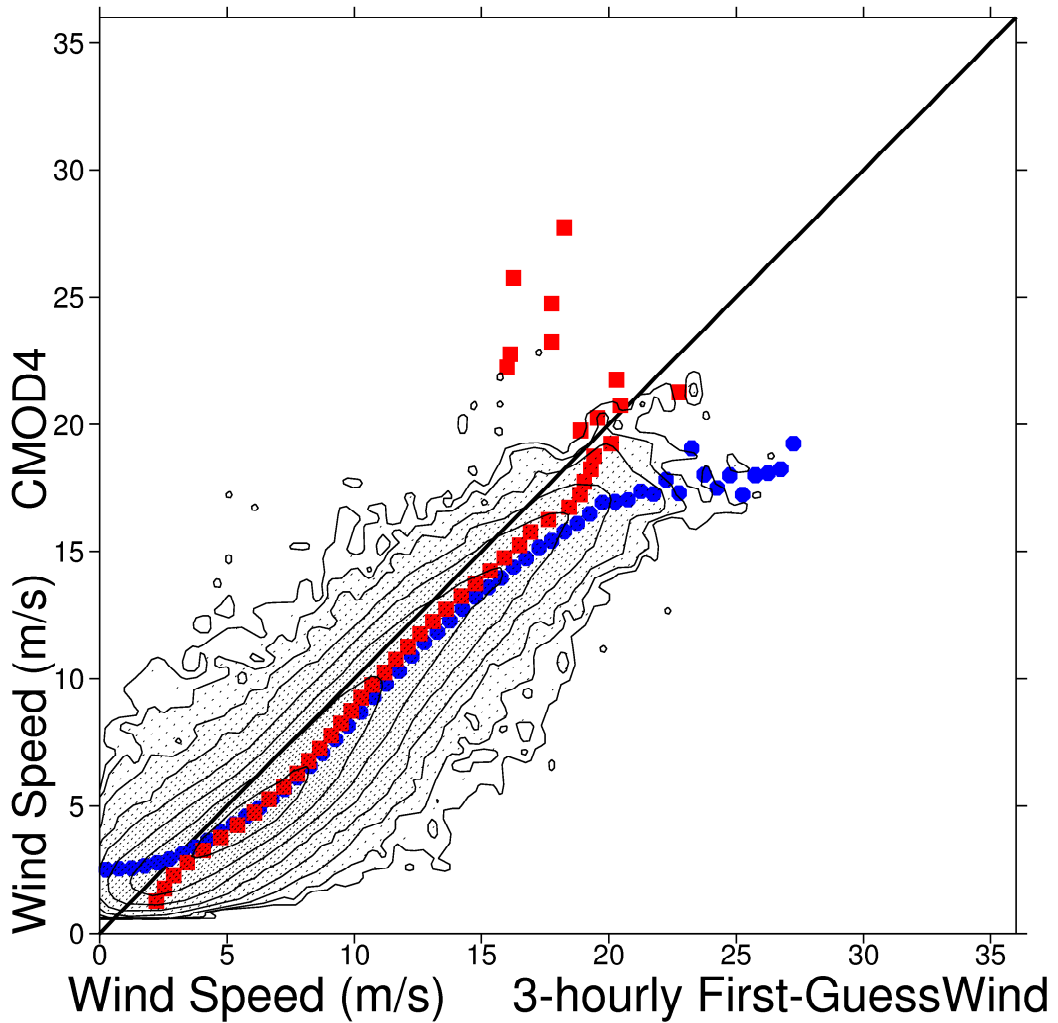


Figure 15

ECMWF 3-hourly First-Guess winds versus CMOD5 winds  
from 2010070600 to 2010080918  
= 546748, db contour levels, 5 db step, 1st level at 2.4 db  
 $m(y-x) = -0.68$   $sd(y-x) = 1.26$   $sdx = 3.34$   $sd_y = 3.23$   $pcxy = 0.963$

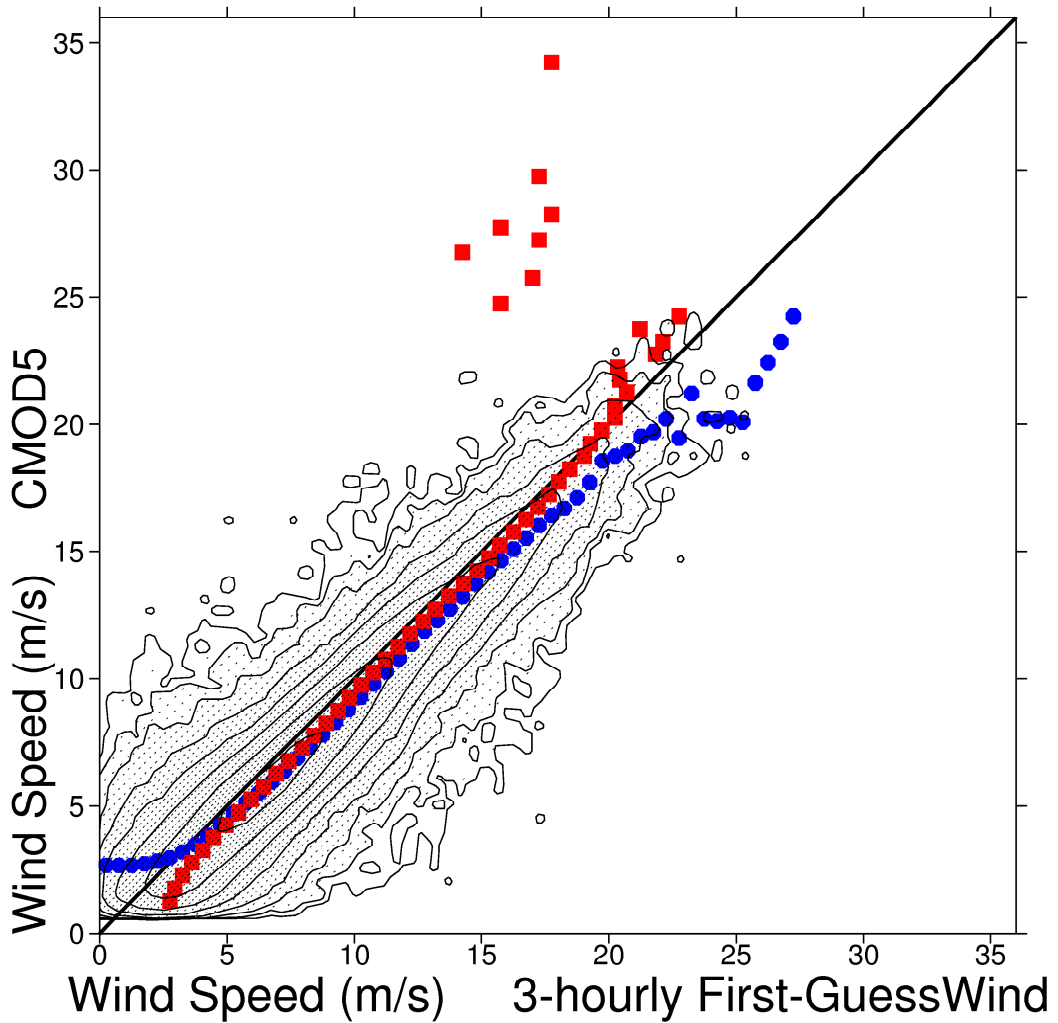


Figure 16